Please replace the paragraph beginning on page 2, line 10 with the following:

--The physical layer configuration is shown in Fig. 1A. At the transmitter, the encoded data stream is sent to an OFDM transmission branch. The data stream may, for example, be convolutionally encoded. The encoded data stream may then be optionally interleaved. If the encoded data stream is interleaved in the transmitter then the receiver must correspondingly deinterleave the data stream. After interleaving, the transmitter modulates the encoded data stream. By way of example, QPSK modulation is used. The signal is then subjected to inverse Fast Fourier Transformation and transmitted, in the present invention over the air.--

Please replace the paragraph beginning on page 9, line 3 with the following:

--In Fig. 2, the performance of the coherent reception with RS code and convolutional codes for 40-Hz maximum Doppler frequency is shown. The convolutional codes are shown with different constraint length (K) ranging from 3 to 9 as dashed lines. The performance of convolutional codes is substantially better than that of the RS code, which is shown as a solid line with cross lines. In order to achieve a Word Error Rate (WER) of 10^{-2}, the K=9 CC needs 4 dB lower SNR than the RS code. In the use of WER in the present invention, it is assumed that a word is a codeword. Moreover, the performance of the K=9 CC with channel estimation is very close to the one with the ideal channel information shown as a solid line.--

Please replace the paragraph beginning on page 9, line 10 with the following:

--In Fig. 3, the performance at 200-Hz Doppler is shown. In comparison with the RS code, the CC's are still superior although the degradation with respect to the idealized case is higher due to poorer channel tracking. In fact, an error floor at the high SNR

region exists due to tracking errors. Once again the RS coded signal is indicated as a solid line with cross lines. The convolutionally coded signals are indicated by dashed lines and ideal channel information is indicated by a solid line.--

Please replace the paragraph beginning on page 9, line 14 with the following:

-- In Fig. 4, the performance of the K=9 CC with different maximum Doppler frequencies is shown. With a low Doppler frequency, a 5-tap (M_l =5) estimator used here can successfully predict the channel and the performance is very close to that with idealized channel estimation. However, when the fading is relatively fast, it is difficult to estimate the channel correctly and the WER floors on the order of 10^{-3} can be clearly observed for at a maximum Doppler frequency of 200 Hz. That is, it was found that the original method works well in slow fading but degrades significantly in fast fading. Once again the ideal Doppler frequency is indicated by a solid line. A Doppler frequency of 200 Hz is indicated by a dashed line. A Doppler frequency of 175 Hz is indicated by a dashed line with small circles. A Doppler frequency of 150 Hz is indicated by a dashed line with triangles and a Doppler frequency of 125 Hz is indicated by a dashed line with cross lines.--

Please replace the paragraph beginning on page 10, line 19 as follows:

--The flowchart of this method is shown in Fig. 1c. The related channel estimation method is first initialized at step 165-1. Transmitted signals are received at step 165-2. A determination is then made at step 165-3 as to whether the received block is a training block. If the received block is a training block then $\hat{c}_n$ is known and

$$\tilde{H}_{m,n} = \arg\min_{H_{m,n}} \sum_m \|x_{m,n} - H_{m,n}\hat{c}_n\|^2$$

is calculated at step 165-5. This is a reference for the channel estimation

3

$$\sum_{l=1}^{M_L} \mathbf{B}_l \mathbf{d}(\widetilde{\mathbf{H}}_{m,n+1-l}) - \mathbf{d}(\hat{\mathbf{H}}_{m,n+1}) = 0$$

which is calculated next at step 165-6. The block number is incremented at step 165-7 and a determination is made if the end of the frame has been reached at step 165-8. If the current block is not a training block then $\hat{\mathbf{c}}_n$ is decoded at step 165-4

$$\hat{\mathbf{c}}_n = \arg\min_{\mathbf{c}_n} \sum_m \|\mathbf{x}_{m,n} - \hat{\mathbf{H}}_{m,n}\mathbf{c}_n\|^2$$

is calculated before calculating the reference and channel estimation.--

Please insert the paragraphs beginning on page 13, after line 23 with the following:

--The physical layer configuration of the system for near optimal joint channel estimation and data detection for COFDM systems is depicted in Fig. 1A. An exemplary transmitter 105 is shown on top and an exemplary receiver 140 is shown on the bottom of Fig. 1A. At transmitter 105, a data stream is accepted by a Convolutional encoder 110, which convolutionally encodes the data stream. The encoded data stream may then optionally be forwarded to an interleaver 115 for interleaving. If the encoded data stream is interleaved in the transmitter 105 then the receiver 140 must correspondingly de-interleave the encoded data stream. After interleaving, a modulator 120, for example a QPSK modulator, modulates the encoded (and optionally interleaved) data stream, which is then forwarded to an inverse Fast Fourier transformer 125, to subject the modulated encoded (and optionally interleaved) data stream to inverse Fast Fourier transformation. The transformed modulated (and optionally interleaved) encoded data stream (signal) is then transmitted, in the present invention, over the air via RF unit 130 and antenna 135.

4

Correspondingly, receiver 140 accepts multicarrier transmitted signals (data streams) via antennas 145 and RF units 150 and subjects the received multicarrier signals to Fast Fourier transformation using Fast Fourier transformers 155. These transformed signals are concurrently fed into channel estimator 165 and demodulators 160, for example QPSK demodulators. The demodulated transformed signals are combined in maximum ratio combiner 170. The combined demodulated transformed are then optionally de interleaved using de-interleaver 175. The combined demodulated transformed (and optionally de interleaved) signal is then decoded using Viterbi decoder 180. The decoded combined demodulated transformed (and optionally de-interleaved) signal is then fed back into channel estimator 165, which forwards channel estimations, which are added to the transformed signals that are forwarded to demodulators 160.

Fig. 1B shows the baseband processing, in particular, the iterative nature of the receiver portion of the system for near optimal joint channel estimation and data detection for COFDM systems. Channel estimator 165 accepts transformed signal 190. Channel estimations 198 are fed back into channel estimator 165. Channel estimations 194 are fed into decoder 185, which comprises maximum ratio combiner 170 (shown in Fig. 1A), optional de-interleaver 175 (shown in Fig. 1A) and Viterbi decoder 180 (shown in Fig. 1A). Channel estimations 195 are fed into decoder 185 via demodulator 160 (shown in Fig. 1A, but not shown in Fig. 1B for clarity and to highlight the iterative nature of the system), which demodulates the transformed signal using channel characteristics. Decoder 185 also accepts transformed signal 190. Decoder 185 outputs signal 192, which is fed back into channel estimator 165.--

Please replace the paragraph beginning on page 15, line 1 with the following:

-- In Fig. 5, the improvement of the system performance is shown. At each time instant n, if the perfect past channel were known, i.e., $[\tilde{\mathbf{H}}_{m,1},,,\tilde{\mathbf{H}}_{m,n-1}] = [\mathbf{H}_{m,1},,,\mathbf{H}_{m,n-1}]$ in (11), the new iterative processing can perform within .3 dB from the case in which channel is known. On the other hand, even if the perfect past channel information was available, the system performance would still be far from the optimal one with an irreducible error floor in the related sub-optimal solution. The SNR requirement of the new iterative approach at a WER of 10^{-2} is 1.2 dB lower than that of the original one. System performance for the original signal is indicated by a dashed line. Using an iterative approach is indicated by a dashed line with triangles. Using the original approach and having perfect past channel information is indicated by a dashed line with circles. Using an iterative approach and having perfect past channel information is indicated by a dashed line with cross lines. The ideal estimate is indicated by a solid line.--

Please replace the paragraph beginning on page 17, line 1 with the following:

-- The iterative channel estimation method depicted in Fig. 6A is first initialized at step 605. The iterative processing for estimating channel characteristics is performed by using the system depicted in Figs. 1A and 1B and as described above. Transmitted signals are received at step 610. A determination is then made as to whether the received block is a training block at step 615. If the received block is a training block then $\hat{c}_n$ is known and

$$\tilde{\mathbf{H}}_{m,n} = \arg\min_{\mathbf{H}_{m,n}} \sum_m \|\mathbf{x}_{m,n} - \mathbf{H}_{m,n}\hat{\mathbf{c}}_n\|^2$$

is calculated, which is a tentative reference signal, by first tentatively decoding the block of the received multicarrier signal at step 620.

The tentative reference signal is then used to generate a tentative estimation for the channel at step 625 given by egn.

$$\sum_{l=1}^{M_L} \mathbf{B}_l \mathbf{d}(\widetilde{\mathbf{H}}_{m,n+1-l}) - \mathbf{d}(\hat{\mathbf{H}}_{m,n+1}) = 0$$

The tentative reference signal is then used to generate a tentative estimation for the channel at step 625 given by at step 635. The block number is incremented at step 630 and a determination is made if the end of the frame has been reached at step 625. If the end of the frame has not been reached then another block of the received multicarrier signal is accepted for processing at step 610. If the current block is not a training block then $\hat{\mathbf{c}}_n$

$$\hat{\mathbf{c}}_n = \arg\min_{\mathbf{c}_n} \sum_m \|\mathbf{x}_{m,n} - \hat{\mathbf{H}}_{m,n}\mathbf{c}_n \|^2$$

is calculated, which is a reference signal, by first decoding the block of the received multicarrier signal at step 640. This reference given by
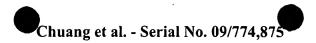
$$\widetilde{\mathbf{H}}_{m,n} = \arg\min_{\mathbf{H}_{m,n}} \sum_m \|\mathbf{x}_{m,n} - \mathbf{H}_{m,n}\hat{\mathbf{c}}_n \|^2$$

is calculated at step 645, which is then used to generate an estimation of channel characteristics given by at step 650.

$$\sum_{l=1}^{M_L} \mathbf{B}_l \mathbf{d}(\widetilde{\mathbf{H}}_{m,n+1-l}) - \mathbf{d}(\hat{\mathbf{H}}_{m,n+1}) = 0$$

The block of the received multicarrier signal is then re-decoded using the estimation of the channel characteristics at step 655. The method then proceeds to the step after determining that the current block is a training block. This effectively repeats the reference and channel estimation. The reference and channel estimation are repeated in

7

order to improve the calculations with the tentative reference and channel estimation

calculations.--

Please replace the paragraph beginning on page 18, line 1 with the following:

-- The iterative backward channel estimation method depicted in Fig. 6B is first

initialized at step 660. The iterative backward processing for estimating channel

characteristics is performed by and using the system depicted in Figs. 1A and 1B and as

described above. Transmitted signals are received at step 665. A determination is then

made as to whether the received block is correct at step 670. If the received block is

correct then $\hat{\mathbf{c}}_n$ is known and

$$\tilde{\mathbf{H}}_{m,n} = \arg\min_{\mathbf{H}_{m,n}} \sum_m \|\mathbf{x}_{m,n} - \mathbf{H}_{m,n}\hat{\mathbf{c}}_n\|^2$$

is calculated, which is a tentative reference signal, by first tentatively decoding the block

of the received multicarrier signal at step 675. This tentative reference signal is then used

to generate a tentative estimation for the channel at step 680 given by.

$$\sum_{l=1}^{M_L} \mathbf{B}_l \mathbf{d}(\tilde{\mathbf{H}}_{m,n+l-1}) - \mathbf{d}(\hat{\mathbf{H}}_{m,n-1}) = 0.$$

The block number is decremented at step 685 and a determination is made if the

beginning of the frame has been reached at step 690. If the beginning of the frame has not

been reached then another block of the received multicarrier signal is accepted for

processing at step 665. If the current block is correct block then $\hat{\mathbf{c}}_n$.

$$\hat{\mathbf{c}}_n = \arg\min_{\mathbf{c}_n} \sum_m \|\mathbf{x}_{m,n} - \hat{\mathbf{H}}_{m,n}\mathbf{c}_n\|^2$$

is calculated, which is a reference signal, by first decoding the block of the received

multicarrier signal at step 692. This reference given by

8

$$\tilde{\mathbf{H}}_{m,n} = \arg\min_{\mathbf{H}_{m,n}} \sum_m \|\mathbf{x}_{m,n} - \mathbf{H}_{m,n}\hat{\mathbf{c}}_n\|^2$$

at step 694 is then used to generate an estimation of channel characteristics at step 696 given by

$$\sum_{l=1}^{M_L} \mathbf{B}_l \mathbf{d}(\tilde{\mathbf{H}}_{m,n+l-1}) - \mathbf{d}(\hat{\mathbf{H}}_{m,n-1}) = 0 .$$

(The block of the received multicarrier signal is then re-decoded using the estimation of the channel characteristics at step 698). The method then proceeds to the step after determining that the current block is correct. This effectively repeats the reference and channel estimation. The reference and channel estimation are repeated in order to improve the calculations with the tentative reference and channel estimation calculations.--

Please replace the paragraph beginning on page 18, line 16 with the following:

-- In Fig. 7, the performance of this approach (iterative backward processing) is shown for 200 Hz maximum Doppler frequency. In the simulation, the maximum M_N is set to be 200 and this corresponds to 40 ms. However, due to the low error probability in the high SNR region, much shorter storage is required. For instance, the maximum M_N required is about 50 at the 5 dB SNR. It is found that nearly optimal performance is achieved with iterative backward processing. System performance using the original approach is indicated by a dashed line. System performance using the iterative approach is indicated by a dashed line with triangles. System performance using the iterative backward processing approach of Fig. 6B is indicated by a dashed line with cross lines. The ideal estimate is indicated by a solid line.--

Please replace the paragraph beginning on page 19, line 4 with the following:

9

-- In Fig. 8, the performance of this approach with different maximum Doppler frequencies is shown. The system still performs well in an environment with maximum Doppler frequency as high as 400 Hz. Once again the ideal estimate is indicated by a solid line. System performance at 500 Hz using iterative backward processing is indicted by a dashed line with crosses (or "x"s). System performance at 400 Hz using iterative backward processing is indicated by a dashed line with small circles. System performance at 300 Hz using iterative backward processing is indicated by a dashed line with triangles. System performance at 200 Hz using iterative backward processing is indicated by a dashed line with cross lines. System performance of the original approach at 200 Hz is indicated by a dashed line.--

Please replace the paragraph beginning on page 19, line 15 with the following:

-- To show the robustness of the iterative approaches, a simple averaging 5-tap finite impulse response FIR filter ($b_l \equiv . 2$) for the time domain filtering is now considered. As shown in Fig. 9, even with these simple FIR coefficients, the method of the present invention still outperforms the original method with the FIR that was optimized for a particular set of maximum Doppler frequency and delay spread. Therefore, the iterative backward-processing approach of the present invention is relatively robust against the mismatch between the FIR coefficients and the true channel. The ideal estimate is indicated by a solid line. System performance using the original approach and an optimal 5-tap FIR at 200 Hz is indicated by a dashed and dotted line. System performance using the original approach and an optimal 5-tap FIR at 40 Hz is indicated by a dashed line. System performance using iterative backward processing and an optimal 5-tap FIR at 200 Hz is indicated by a dashed line with crosses (or "x"s).

10

System performance using iterative backward processing and an optimal 5-tap FIR at 40 Hz is indicated by a solid line with crosses (or "x"s).--

Please replace the paragraph beginning on page 21, line 16 with the following:

-- First consider K=5 and 40 Hz or K=9 and 125 Hz based on the related/original (non-iterative) method, both give similar link performance (see Figs. 2 and 5), for a comparison between RS and CC coding methods. Fig. 10 shows the average probability of packet retransmission, as a function of occupancy for all available (24) channels in each sector. This is a measure of QoS (quality of service) experienced by individual users. With a 3-6 % target retransmission probability, 15-50 % occupancy per radio in each sector is possible with this DPA scheme, depending on the use of coding schemes. Clearly, joint channel estimation and maximum likelihood detection of CC indicated by a dashed line introduced previously provides significant improvement over the case of RS codes, indicated by a solid line with cross lines which is also similar to the case of differential demodulation of the RS codes with 4 transmit antennas. Both results are significantly superior to the efficiency provided by current cellular systems, which are typically designed for voice communications with very conservative frequency reuse, about 4-7% spectrum occupancy in each sector. Data applications, permitting some retransmission delay, and improved link design, introduced here, allow much more aggressive and efficiency frequency reuse.--

Please replace the paragraph beginning on page 22, line 8 with the following:

-- Fig. 11 shows that 1-1.5 Mb/s can be successfully delivered by each base station with an average delay on the order of 40-120 msec. This is a measure for system capacity. It indicates that OFDM link and DPA MAC combined enable a spectrally efficient (40%-60% b/s/Hz with a conservative assumption of overhead requirements) air interface for broadband services, even for the macrocellular environment considered here. Adaptive modulation has not been considered in this study, and its use is expected to improve efficiency beyond 1 b/s/Hz per base station even under aggressive frequency reuse. The OFDM technology discussed herein can provide robust performance with peak-rates scalable with the available bandwidth. RS codes are indicated by a solid line with cross lines. CC codes are indicated by a dashed line.--

Please replace the paragraph beginning on page 22, line 16 with the following:

-- Next, consider the case of high maximum Doppler frequency (200 kHz) and K=9 (WER curves in Fig. 6) for comparison between sub-optimal ("original") detection method discussed earlier and near-optimal iterative backward-processing method presented. Fig. 12 shows that retransmission probability using the improved method can work well even under high maximum Doppler frequency. As a result, QoS can be improved even for high mobility users or when higher carrier frequency is employed. System performance using the original detection method is indicated by a solid line with cross lines. System performance using the iterative backward processing approach is indicated by a dashed line. On the other hand, the capacity difference is relatively smaller, as shown by the delay-throughput curves in Fig. 13. System performance using the original approach is indicated by a solid line with cross lines and system performance